Electronic Supplementary Material (ESI) for Journal of Materials Chemistry C.

Supplementary Information

Highly pure pentacene crystals grown by physical vapor transport: the critical role of the carrier gas

Hye Soo Kim,[a] Soyoung Kim,[b] Jin Young Koo[b] and Hee Cheul Choi*[b]

[a]*Division of Advanced Materials Science, Pohang University of Science and Technology (POSTECH), Pohang 37673, Republic of Korea*

[b]*Department of Chemistry, Pohang University of Science and Technology (POSTECH), Pohang 37673, Republic of Korea*

E-mail: choihc@postech.edu

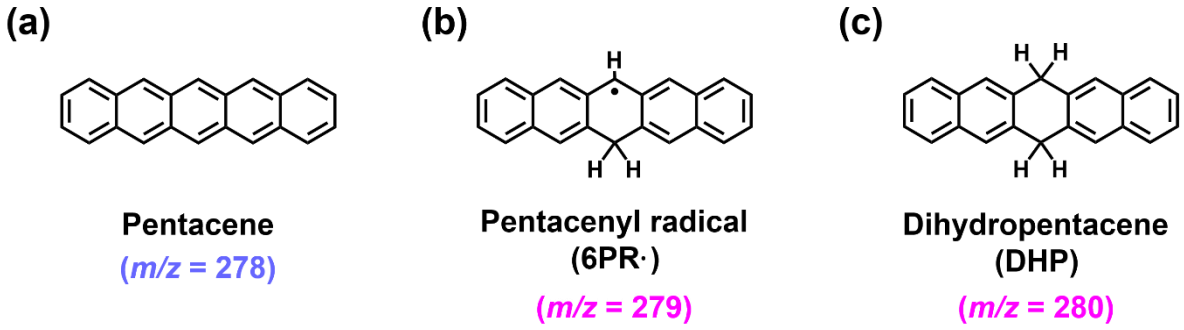

Fig. S1. Molecular structures of (a) pentacene, (b) pentacenyl radical (**6PR**), and (c) dihydropentacene (**DHP**).

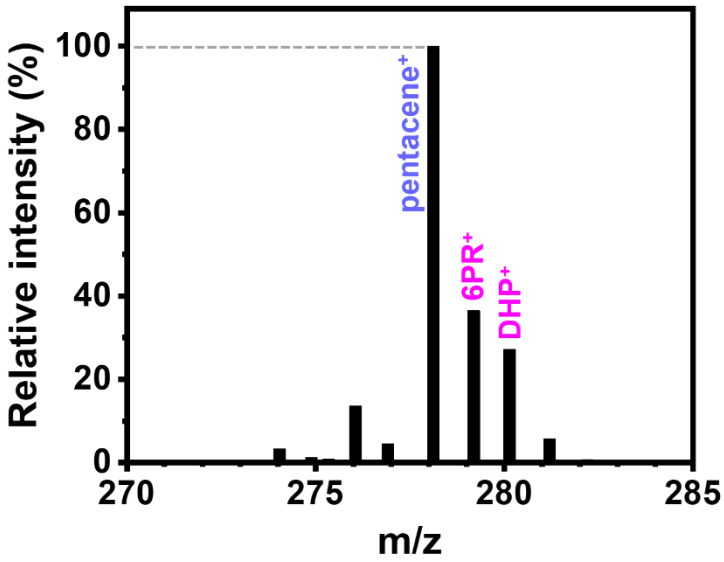

Fig. S2. Mass spectrum of commercial pentacene powder (Sigma-Aldrich). It is expressed as a relative intensity in % between *m/z*=270 and 285, based on pentacene at *m/z*=278. A relatively large amount of *m/z* at 279 and 280 indicates the presence of impurities with similar molecular weights of pentacene, such as **6PR** and **DHP**.

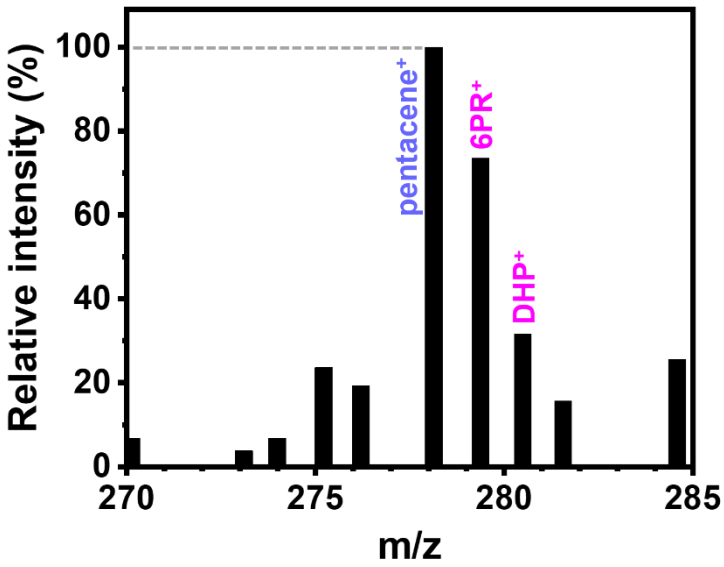

Fig. S3. Mass spectrum of pentacene powder after annealed at 503 K for 60 minutes in an inert environment. Upon heating, it shows an increase of the impurities, compared to 298 K (without further treatment).

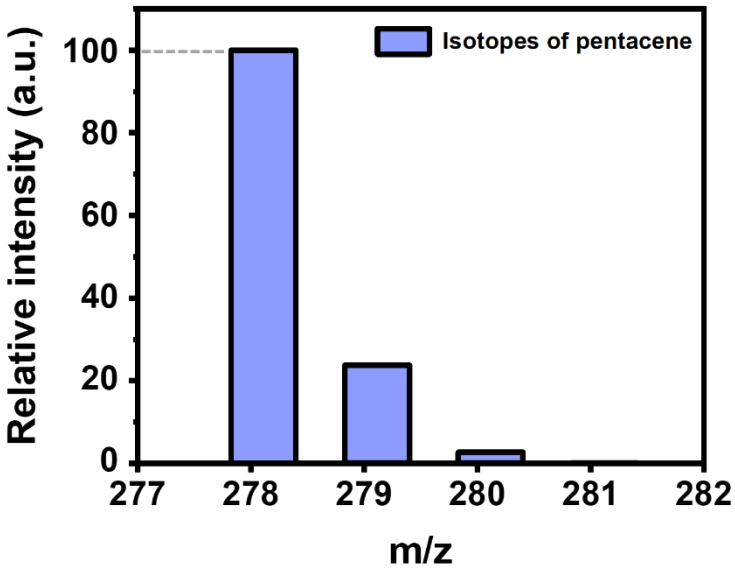

Fig. S4. Calculated mass spectrum of isotopic pentacene ($C_{22}H_{14}$).

(a)

$$v_{r.m.s.} = \sqrt{\frac{3RT}{M}}$$

$v_{r.m.s.}$ = **Root mean square velocity of the gas**
R = Gas constant
T = Absolute temperature
M = Molecular weight of the gas

(b)

	Molecular weight (g mol^{-1})	$v_{r.m.s.}$ (m s^{-1})
Ar	39.94	623.7
H_2	2.016	2776
N_2	28.01	744.8
He	4.003	1970

Fig. S5. Kinetic parameters of various carrier gases at 625 K. (a) Equation of root mean square velocity defined by the molecular weight of gas and temperature. (b) Comparison of the molecular weight and the average velocity of gases. The velocity of H_2 is 4.5 times faster than that of Ar as molecular weight is inversely proportional to the velocity of each gas molecule. In accordance with similar molecular weight, Ar-N_2 and H_2-He have a similar trend in the velocity.

(a)

$$Ra = \frac{g\beta\Delta T d^3}{\nu\alpha}$$

***Ra* = Rayleigh number**

g = Acceleration of gravity
d = Characteristic length of the tube
β = Thermal expansion coefficient
ν = Kinematic viscosity
ΔT = Temperature difference
α = Thermal diffusivity

(b)

	β (K^{-3})	ν ($10^{-4}m^2/s$)	α ($10^{-4}m^2/s$)	***Ra***
Ar	1.661	22.06	0.22	60,913
H_2	0.0899	163.8	1.9	1,128
N_2	1.165	23.94	0.22	56,132
He	0.1664	181.0	1.6	859.6

Fig. S6. Equation and parameters for Rayleigh number (***Ra***). (a) Equation of dimensionless Rayleigh number defined by thermofluid parameters, such as viscosity and thermal diffusivity. (b) Comparison of Rayleigh numbers of carrier gases, which determine the flow type in a quartz tube. As the convective flow becomes dominant for larger Rayleigh number than 1,296 (critical Rayleigh number). Ar-N_2 and H_2-He show similar trends of convective flow and laminar flow, respectively.

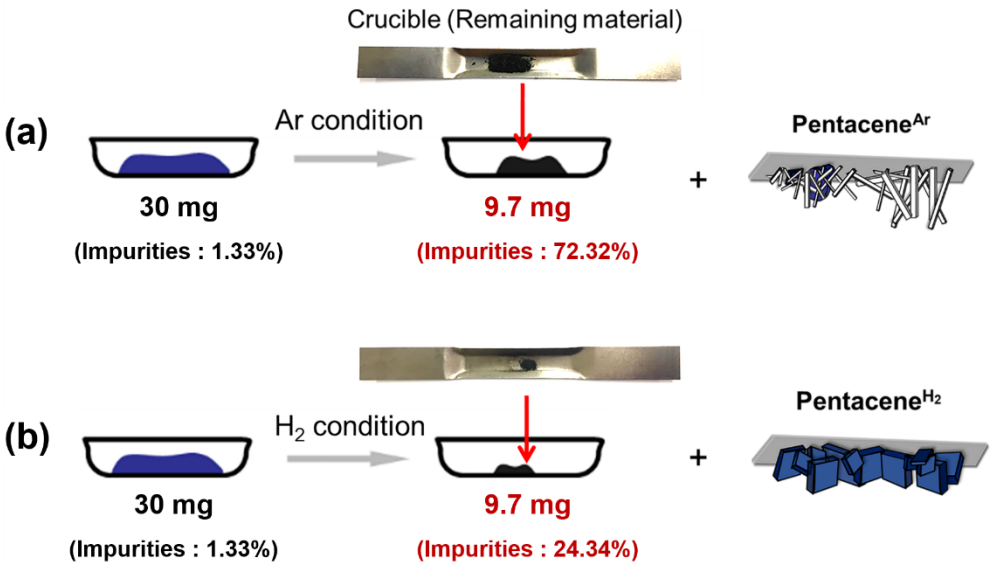

(c)

Condition	Impurities of the remaining material after crystal growth		
	Type	Percentage	
Ar	6PR	21.36%	72.32%
	DHP	32.22%	
	PP	18.74%	
H_2	6PR	8.18%	24.34%
	DHP	15.52%	
	PP	0.64%	

Fig. S7. The differences of remaining materials and products grown in Ar and H_2 environments. (a, b) Summary of PVT reactions from starting materials to residue in the crucible in (a) Ar and (b) H_2 environment. (c) The composition and percentage ratio of remaining impurities after crystal growth. In the Ar environment, the impurities increased by about 3.7 mg compared to before the reaction, whereas in the H_2 environment, only 0.08 mg increased. These results clearly show that the formation of impurities is well suppressed under the H_2 environment.

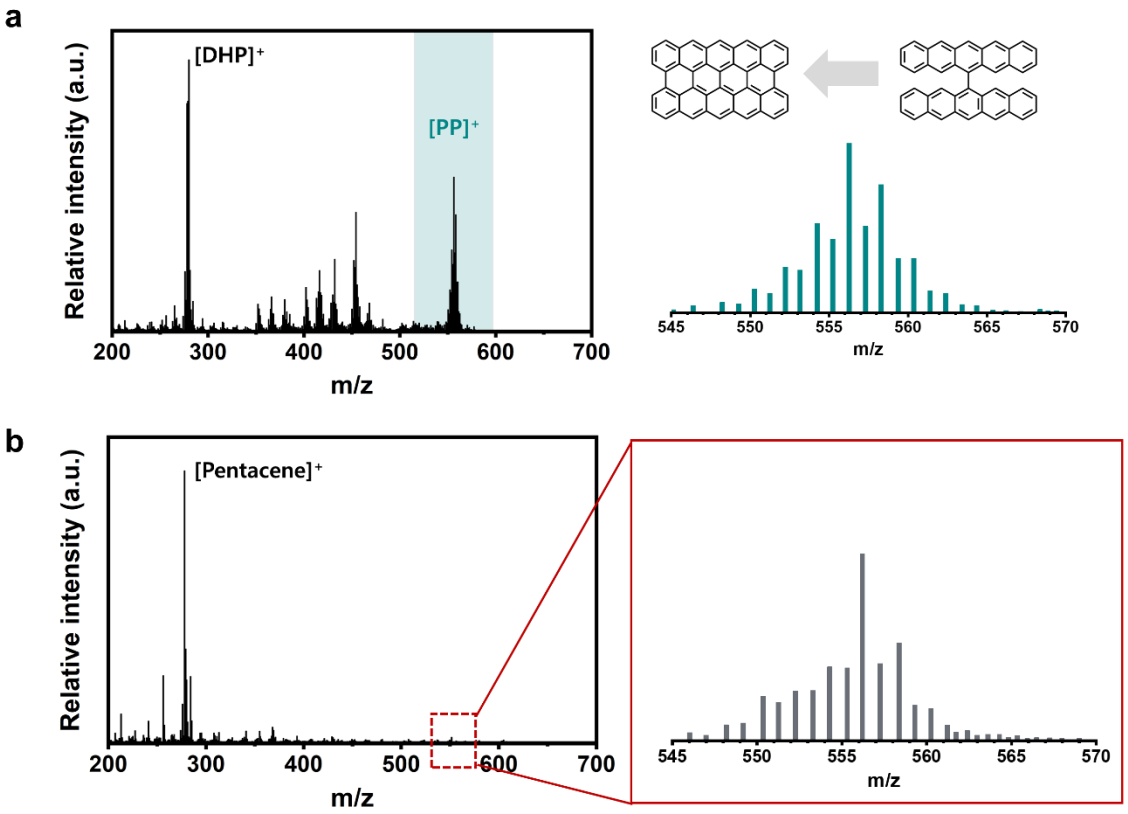

Fig. S8. Mass spectra of the residue in (a) Ar and (b) H_2 which consists of the distribution of *m/z* peaks occurring in the hydrogenation from bipentacene to fully fused **PP**. The intensity ratio of **PP** to pentacene in Ar environment remains much larger than in H_2 environment. Hence, the disproportionation reaction rarely occurs in H_2 environment, while it occurs actively in Ar environment.

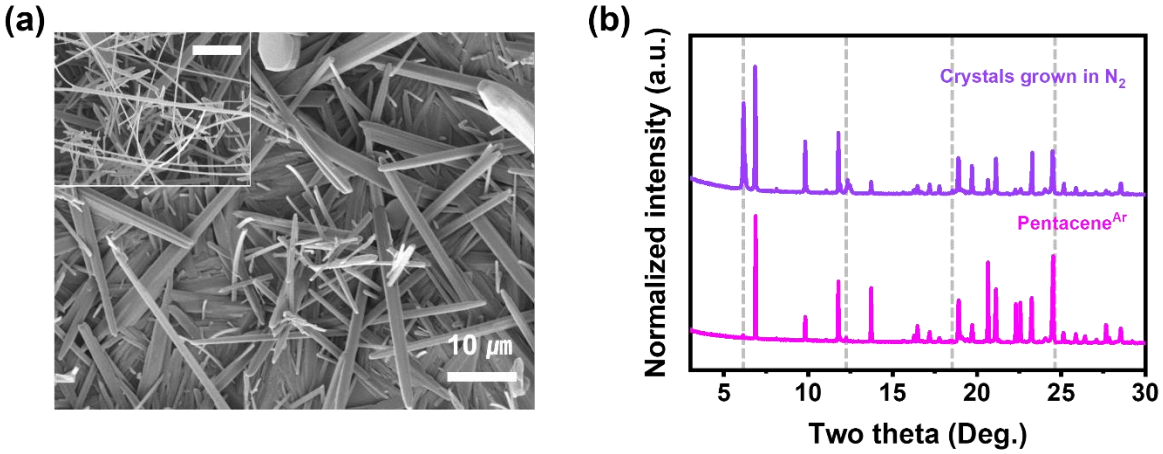

Fig. S9. (a) SEM image and (b) PXRD pattern (purple) of resulting crystals grown in N_2 environment. The PXRD pattern is almost identical to that of pentacene^{Ar} (magenta), which indicates the formation of DHP-pentacene cocrystal. It should be noted that the peaks with two theta values of ~6°, 12°, 18°, and 24° (grey with dashed line) come from plate-shaped pentacene crystals.

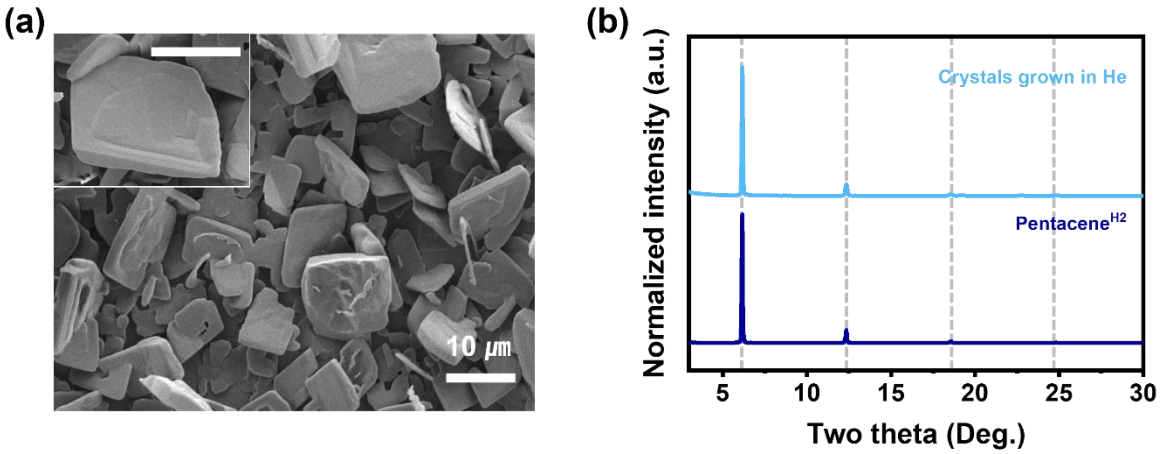

Fig. S10. (a) SEM image and (b) PXRD pattern (sky-blue) of the resulting crystals grown in He environment. The diffraction pattern of pentacene^{H2} (blue) is identical to that of pentacene^{H2} having two theta values of ~6°, 12°, 18°, and 24° (grey with dashed line).

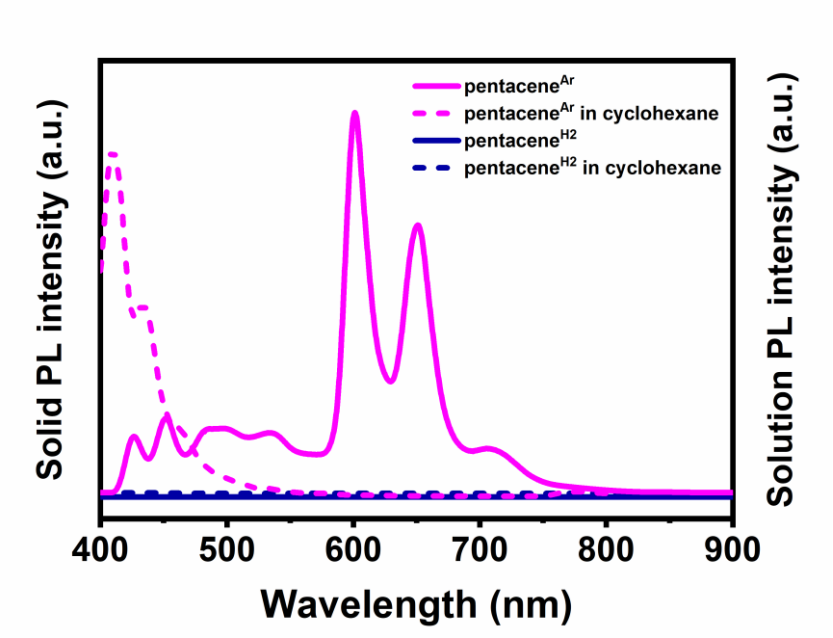

Fig. S11. PL properties of pentacene^{Ar} and pentacene^{H2} in the aggregate and solution states measured at 298 K; while pentacene^{Ar} is still highly emissive in solution state, pentacene^{H2} is non-emissive.

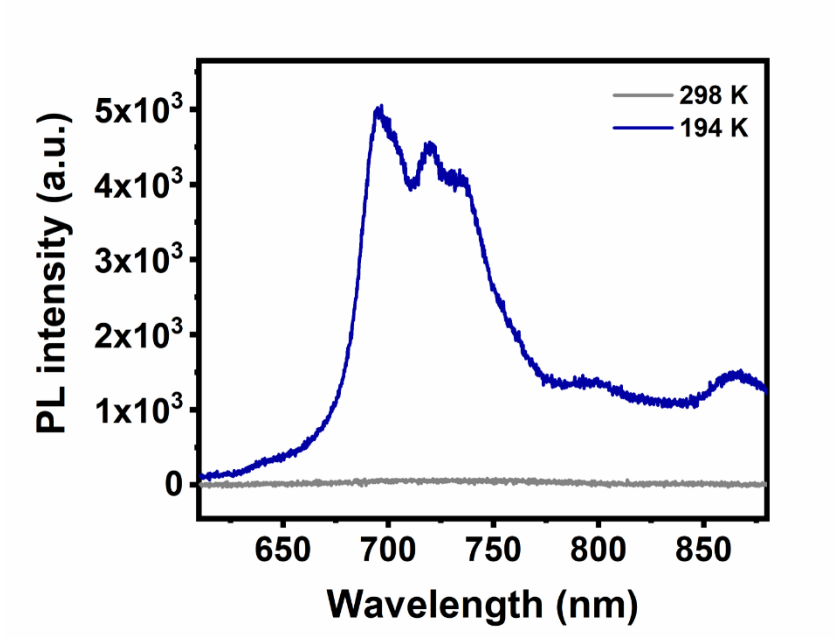

Fig. S12. PL spectra of pentacene^{H2} measured at 298 K (grey) and 194 K (blue).

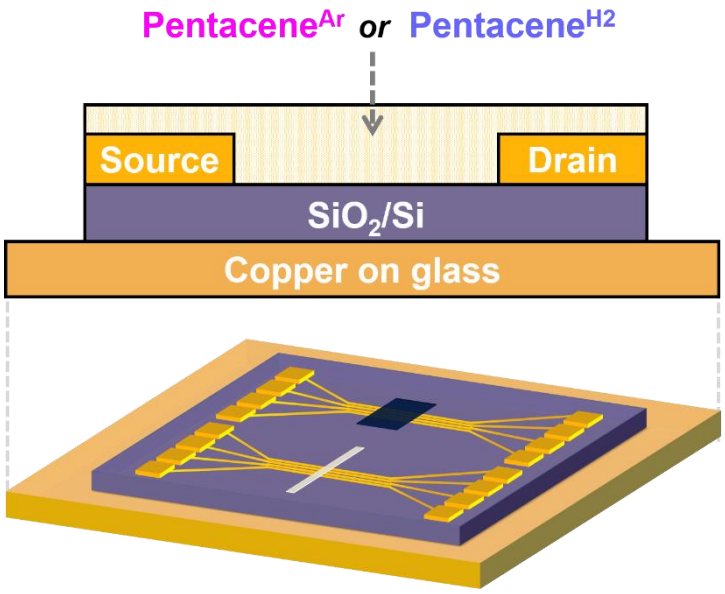

Fig. S13. Schematic of the field-effect transistor (FET) device.

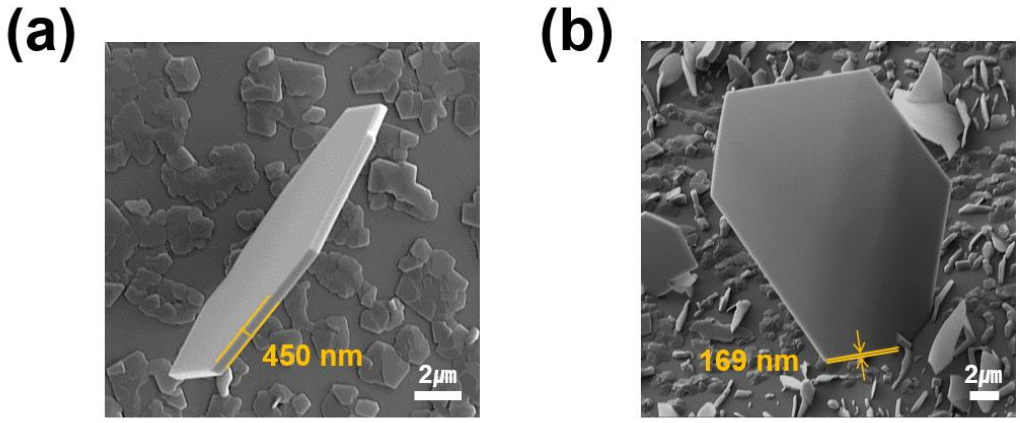

Fig. S14. Pentacene^{H2} with controlled thicknesses for fabricating OFET devices. (a, b) SEM images of pentacene^{H2} obtained from; (a) original condition and (b) modified condition of PVT.

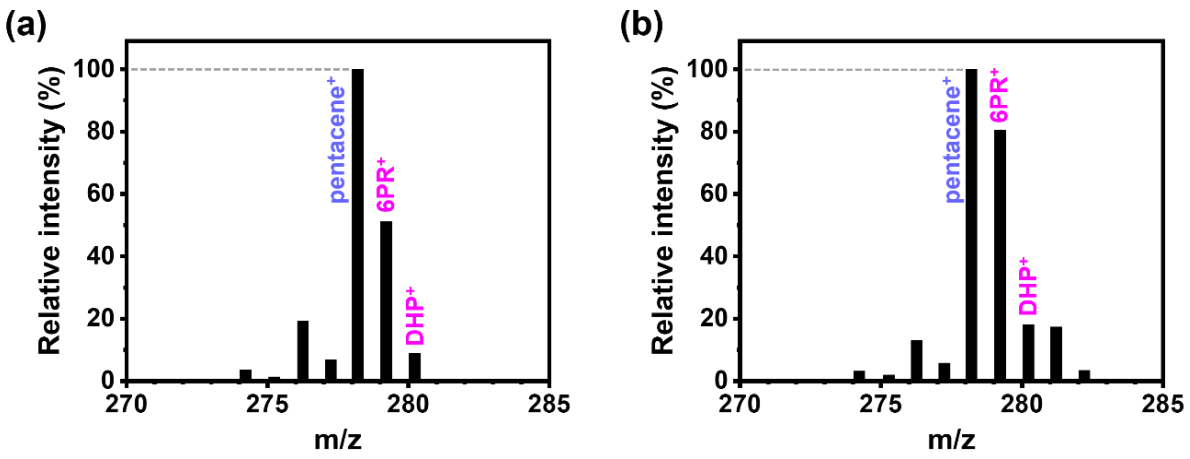

Fig. S15. Mass spectra of commercially available pentacene powder (TCI (Japan)) with (a) no further treatment and (b) thermal annealing at 503 K for 60 min under Ar flow. Like as pentacene powder purchased from Sigma-Aldrich, a drastic increase in peak intensities of the impurities (**6PR** and **DHP**) is shown by heat.

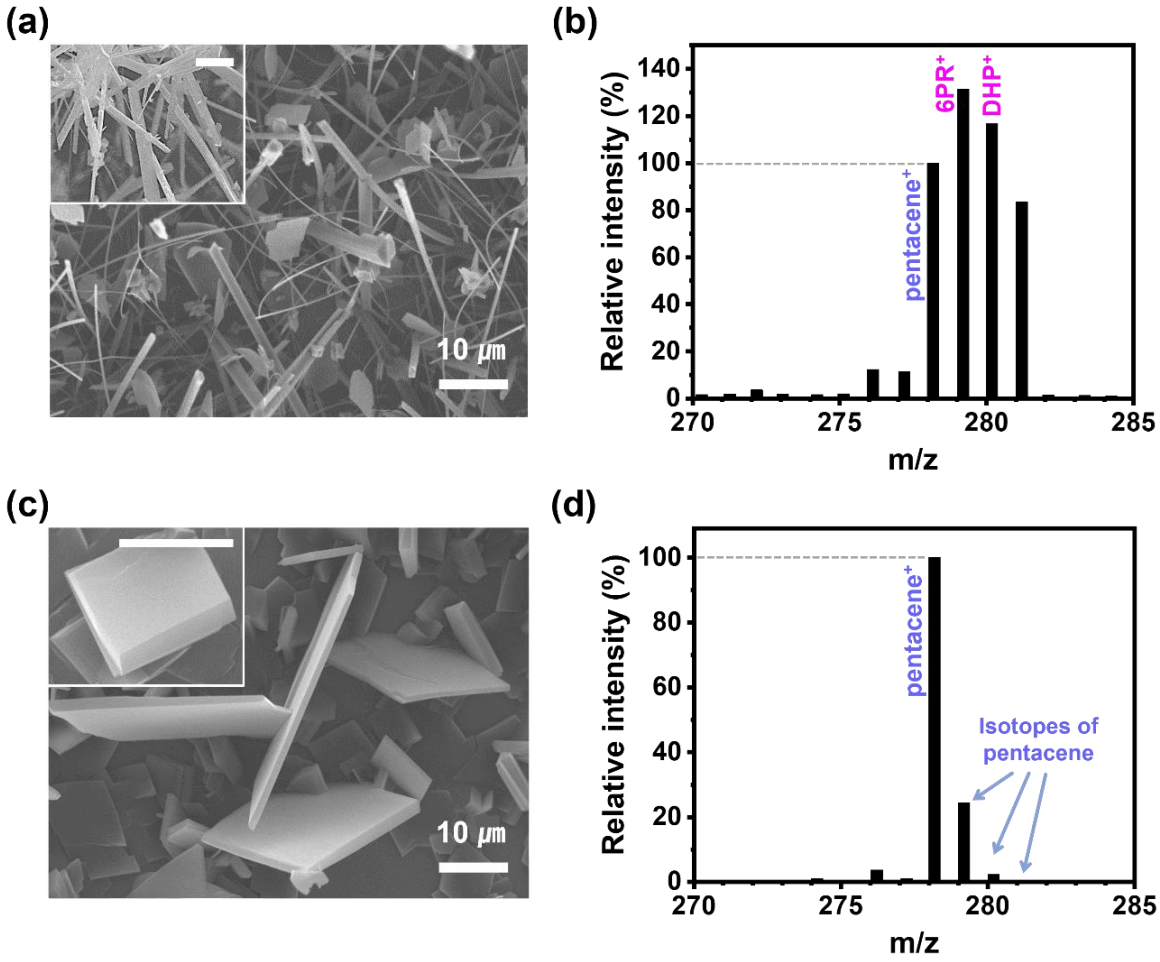

Fig. S16. SEM images and mass spectrum of (a, b) pentacene^{Ar} and (c, d) pentacene^{H2} grown using pentacene powder purchased from TCI (Japan). The scale bar in the inset image is 10 μm.

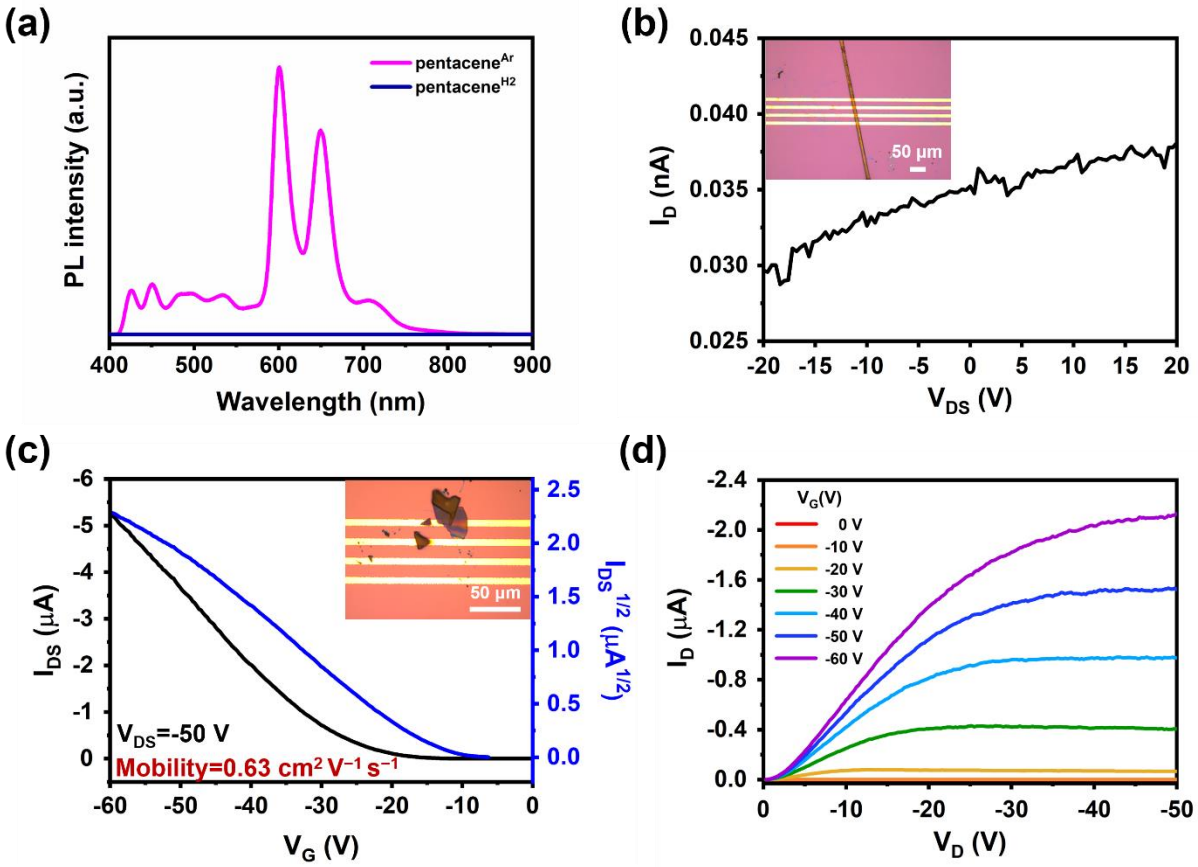

Fig. S17. PL and electrical properties of pentacene^{Ar} and pentacene^{H2}. (a) PL spectra of pentacene^{Ar} (magenta) and pentacene^{H2} (blue). (b) *I-V* characteristics of insulating pentacene^{Ar}. (c, d) Transfer and output curves of pentacene^{H2} indicating *p*-type semiconducting behavior.

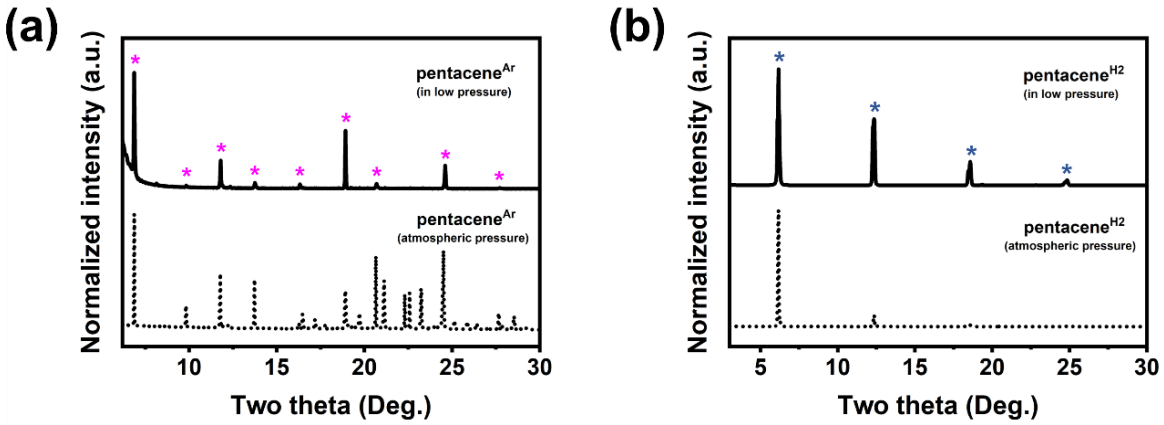

Fig. S18. PXRD patterns of resulting crystals grown in (a) Ar and (b) H_2 environments at low pressure. The PXRD result of (a) pentacene^{Ar} and (b) pentacene^{H2} grown at low pressure is almost identical to that of pentacene^{Ar} and pentacene^{H2} grown at atmospheric pressure (dots), respectively.